

FDTD ANALYSIS OF DIPOLE ANTENNA AS EMI SENSOR

M. Ali and S. Sanyal

Dept. of Electronics & Electrical Communication Engineering
Indian Institute of Technology
Kharagpur-721 302, India

Abstract—Electromagnetic Interference (EMI) is becoming a crucial issue in the era of modern electronic systems. For EMI measurement, it is required to place a sensor to receive the radiation from the equipment in a suitable test environment. The performance of the sensor depends on its Antenna Factor, which is the ratio of the incident electric field on the antenna surface to the received voltage at the load end across $50\ \Omega$ resistance. FDTD is one of the efficient numerical techniques to solve radiation and scattering problem in any environments. To the best of the knowledge of the authors no literature is available where FDTD is used to evaluate the Antenna Factor. Here, in this work we applied FDTD to predict the performance of dipole antenna when it is used as a EMI sensor. The results presented here for free space environment are compared with published results.

1. INTRODUCTION

All the electronic devices must conform to the standards of electromagnetic emission set by different bodies in different countries. The frequency range of conducted emission standards extend from 450 KHz to 30 MHz and for that radiated emissions begins at 30 MHz and extends to 40 GHz [1]. Compliance of the devices conforming to the standards (limits) of interference in this range is verified by measuring the radiated electric fields in an anechoic chamber or at an open test range after putting the measurement antenna at a specified distance from the device under test. Wire antennas are widely used as transmitting antenna and as sensor for electromagnetic interference (EMI) measurements. The term wire refers to metallic, highly conducting wire or wire-like structures.

FDTD is one of the efficient numerical techniques to solve Maxwell's equations in any environments. To the best of author's knowledge no appreciable work is available on this area. In this work our attention is concentrated on the characterization of the wire antennas as EMI sensors in terms of the Antenna Factor using FDTD methods.

For EMI measurement it is required to determine the field strength at the point of measurement using a sensor. To use the sensor for this purpose, calibration data is required relating the electric field at the aperture of the receiving antenna to the voltage at the $50\ \Omega$ matched detector. The most common performance descriptor of EMI sensors is the Antenna Factor. The ratio of the incident electric field on the surface of the sensor to the received voltage at the antenna terminal when terminated with a $50\ \Omega$ load is known as the Antenna Factor [1].

In this work the Finite Difference Time Domain (FDTD) technique has been used to evaluate the current distribution on the dipole antenna surface when it is illuminated by the plane wave and subsequently calculate the voltage and hence Antenna Factor of the dipole antenna. For the validation of the theory, computed Antenna Factor of a dipole was compared with the published results. First case a simple dipole antenna was taken and compared the FDTD computed result with MoM results, published in result [2]. Secondly the Antenna Factor of a ANRITSU MP651A dipole obtained using FDTD technique was compared with the data available from the instruction manual. Finally the Antenna Factor of a broadband dipole (i.e., dipole top and bottom loaded with circular disc) obtained using FDTD technique was compared with the data available in the literatures [3, 4].

1.1. FDTD Formulation of the Problem

The Finite Difference Time Domain method(FDTD) has been widely accepted as a reliable computational tool in numerical electromagnetic. The explicit nature of the time-stepping algorithm to solve Maxwell's equations conveniently enables the visualization of the electromagnetic fields inside the medium under investigation. This feature is a great benefit compared to frequency-domain methods, like the Method of Moments (MOM) or the Finite-Element Method (FEM).

The original FDTD paradigm was described by Yee cell, named, of course, after Kane Yee [5]. Let E and H field are assumed interleaved around a cell whose origin is at the location i, j, k . Every E field is located $1/2$ cell width from the origin in the direction of its orientation; every H field is offset $1/2$ cell in each direction except that of its orientation.

Starting with Maxwell's equations [6]:

$$\frac{\partial \tilde{D}}{\partial t} = \frac{1}{\sqrt{\epsilon_0 \mu_0}} \vec{\nabla} \times \vec{H} \quad (1a)$$

$$\tilde{D} = \epsilon_r^*(\omega) \cdot \tilde{E} \quad (1b)$$

$$\frac{\partial \vec{H}}{\partial t} = -\frac{1}{\sqrt{\epsilon_0 \mu_0}} \vec{\nabla} \times \tilde{E} \quad (1c)$$

where, $\epsilon_r^*(\omega)$ is the complex relative dielectric constant. \tilde{D} and \tilde{E} are the normalized value of the corresponding field components given by,

$$\tilde{D} = \sqrt{\frac{\epsilon_0}{\mu_0}} \vec{D} = f_n \cdot \vec{D} \quad (2a)$$

$$\tilde{E} = \sqrt{\frac{\epsilon_0}{\mu_0}} \vec{E} = f_n \cdot \vec{E} \quad (2b)$$

f_n is the normalized factor given by,

$$f_n = \sqrt{\frac{\epsilon_0}{\mu_0}} \quad (3)$$

The notation \sim is dropped, but it will always be assumed that we are referring to the normalized value. The electric field components are

$$E_x = gax \cdot D_x \quad (4a)$$

$$E_y = gay \cdot D_y \quad (4b)$$

$$E_z = gaz \cdot D_z \quad (4c)$$

where,

$$gax = \frac{1}{\epsilon_r + \frac{\sigma \Delta t}{\epsilon_0}} \quad (5)$$

Expression of gay & gaz is same as for gax [6] in Eqn. (5).

Where,

- ϵ_0 is the free space permittivity.
- μ_0 is the free space permeability.
- ϵ_r is the relative permittivity of the medium.
- σ is the conductivity of the medium.

- Δt is the time increment.

All of the information regarding the medium is contained in Eqn. (4). For free space, $g_{ax} = g_{ay} = g_{az} = 1$; for PEC $g_{ax} = g_{ay} = g_{az} = 0$ and for lossy material, g_{ax} , g_{ay} , & g_{az} are calculated according to Eqn. (5).

In the FDTD method we solve the Eqns. (1a) and (1c) simultaneously using central difference approximations for both the temporal and spatial derivatives.

To ensure the accuracy of the computed results, the spatial increment δ must be small compared to the wavelength (*usually* $\leq \lambda/10$) or minimum dimension of the scatterer. This amounts to having 10 or more cells per wavelength. To ensure the stability of the finite difference scheme of Eqn. (1a) and (1c) the time increment Δt must satisfy the following stability condition [7, 8]

$$u_{max} \Delta t \leq \left[\frac{1}{\Delta x^2} + \frac{1}{\Delta y^2} + \frac{1}{\Delta z^2} \right]^{-1/2} \quad (6)$$

where u_{max} is the maximum wave phase velocity within the model. Since we are using a cubic cell with $\Delta x = \Delta y = \Delta z$, the time step Δt is determined by ‘‘Courant Condition’’ [9, 6] and details of Eqn. (6) is given by

$$\Delta t \leq \frac{\Delta x}{\sqrt{n} \cdot c_0} \quad (7)$$

where, c_0 is the speed of light in free space and n is the number of space dimensions. For practical reasons, it is best to choose the ratio of the time increment to spatial increment as large as possible yet satisfying Eqn. (7). Though it is not necessarily the best formula; however, we will use it for simplicity.

$$\frac{1}{\sqrt{\epsilon_0 \mu_0}} \frac{\Delta t}{\Delta x} = c_0 \frac{\Delta x/2 \cdot c_0}{\Delta x} = \frac{1}{2} \quad (8)$$

A 15Δ -thick unsplit Perfectly Matched Layer (PML) [6, 10, 11] is used as Absorbing Boundary Condition (ABC) on all six sides of the FDTD lattice. This PML is spaced 4Δ cells from the closest surface of the source or scatterer.

The excitation source is set up by assigning a desired time function to specific electric or magnetic field components in the FDTD space lattice. In this study, the time function Gaussian pulse is taken as a hard source.

Hard source is set up by forcing a desired time function to the E_z components in the $abcd$ plane. For Gaussian input pulse, the E_z component in the $abcd$ plane at time step t is given by

$$E_{z_{i,j,k}}^t = A e^{-0.5 \cdot \left(\frac{t-t_0}{t_\omega}\right)^2} \quad (9)$$

where, t_ω is the standard deviation and relates the line width at half-height by the relationship

$$t_{1/2} = \sqrt{8 \ln(2)} \cdot t_\omega = 2.35482 \cdot t_\omega \quad (10)$$

FDTD is a time domain technique so to get frequency domain data we have to use Fourier transformations [6]. We iterate the FDTD program until the pulse has died out, and take the Fourier transform of the field components in the slab. Fourier transform of the E -field $E(t)$ at a frequency f_1 is

$$E(f_1) = \int_0^{t_T} E(t) \cdot e^{-j2\pi f_1 t} dt. \quad (11)$$

Notice that the lower limit of the integral is 0 because the FDTD program assumes all causal function. The upper limit of the integral is t_T , the time at which the FDTD iteration is halted. Rewriting Eqn. (11) in the finite difference form,

$$E(f_1) = \sum_{n=0}^T E(n \cdot \Delta t) \cdot e^{-j2\pi f_1 (n \cdot \Delta t)} \quad (12)$$

where T is the number of iterations and Δt is the time step, so $t_T = T \cdot \Delta t$.

1.2. Total/Scattered Field Formulation

To calculate the far field antenna factor we have to illuminate the antenna by a plane wave. So first we have to simulate a perfect plane wave within the problem space. In order to simulate a plane wave in a FDTD program, the problem space will be divided up into region, the total field and scattered field [6]. Details of the method given in [6], is used in this work.

1.3. Modeling of Dipole Antenna

A simple dipole antenna is illustrated in Fig. 1, consists of two metal arms. A dipole antenna functions by having current run through

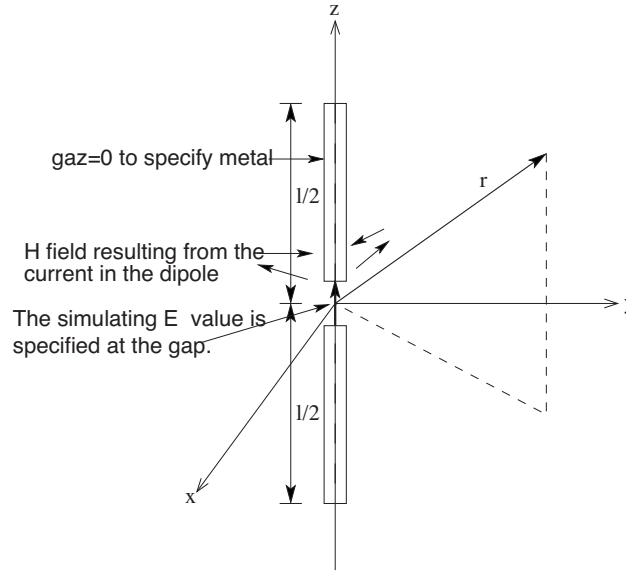


Figure 1. A dipole antenna. The FDTD program specifies the arms of the dipole by setting $g_{az} = 0$. The source is specified by setting the E_z field to a value at the gap.

the arms, which results in radiation. FDTD simulates a dipole in the following way: The metal of the arms is specified by setting the g_{az} parameters of Eqn. (4) to zero in the cells corresponding to the metal except the place where source is placed. This insures that the corresponding E_z field at this point remains zero, as it would if that point were inside metal. The source is specified by setting the E_z field in the gap to a certain value.

For the FDTD simulation, dipole is fed at the center ($x = i_s \Delta x$, $y = j_s \Delta y$, $z = k_s \Delta z$) gap of length Δz with a Gaussian pulse of $A=1.0$ V maximum amplitude as in Eqn. (9). So, electric field in the gap of the dipole is

$$E_z|_{i_a, j_a, k_a + 1/2}^n = -\frac{V(n \Delta t)}{\Delta z} \quad (13)$$

The current in the wire at the feed point is obtained by applying Ampere's law [9] to the surface S with the bounding contour C on the wire at $(i_s, j_s, k_s + 3/2)$:

$$\oint_C \vec{H} \cdot d\vec{L} = \iint_S \vec{J} \cdot d\vec{S} + \epsilon_0 \iint_S \frac{\partial \vec{E}}{\partial t} \cdot d\vec{S} \quad (14)$$

This gives the current:

$$I|^{n+1/2} = \Delta x \left(H_x|_{i_a, j_a-1/2, k_a+3/2}^{n+1/2} - H_x|_{i_a, j_a+1/2, k_a+3/2}^{n+1/2} \right) \cdot f_n \\ + \Delta y \left(H_y|_{i_a+1/2, j_a, k_a+3/2}^{n+1/2} - H_y|_{i_a-1/2, j_a, k_a+3/2}^{n+1/2} \right) \cdot f_n \quad (15)$$

Where, f_n is the normalized factor, given in the Eqn. (3). From the Lee's algorithm, we can write

$$I|^{n+1/2} = f_n \Delta x \left(H_x|_{i_a, j_a-1, k_a+1}^{n+1/2} - H_x|_{i_a, j_a, k_a+1}^{n+1/2} \right) \\ + f_n \Delta y \left(H_y|_{i_a, j_a, k_a+1}^{n+1/2} - H_y|_{i_a-1, j_a, k_a+1}^{n+1/2} \right) \quad (16)$$

1.4. Antenna Factor

1.4.1. Introduction

To carry out field strength measurements, one typically connects an antenna to a spectrum analyzer or some other type of receiver. The Antenna Factor (\overline{AF}) is the parameter that is used to convert the voltage or power reading of the receiver to the field strength incident on the antenna [13, 14]. In terms of an equation, the (\overline{AF}) is defined [15] as

$$\overline{AF} = \frac{\text{Incident electric field } (\vec{E}_i)}{\text{Received voltage } (V)} \quad (17)$$

where \vec{E}_i is the electric field incident on the antenna, and V , is the voltage induced across a 50Ω load at the feed point of the antenna.

Figure 2 is an illustration of the problem space of a 3-D FDTD program. The FDTD model uses a uniform space lattice cubic Yee cells. A dipole (along z -axis) is illuminated by a z -directed linearly polarized plane wave. The time domain current $I(t)$ flowing through the center of the dipole is calculated using Eqn. (16). During the progress of the FDTD calculations this field $E_z(t)$ and current $I(t)$ are saved for each time step. The FDTD calculation are continued until all transients are dissipated, so that the Fourier transform yields the steady-state frequency domain response of the antenna. Fourier transform of the current $I(t)$ gives frequency domain current $I(\omega)$ flowing through the center of the dipole. Voltage developed across 50Ω load is $V(\omega) = 50 \cdot I(\omega)$. Finally antenna factor of the dipole antenna is evaluated using Eqn. (17).

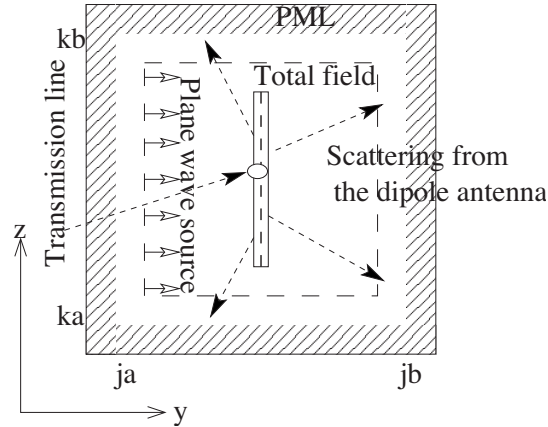


Figure 2. Receiving antenna case. Dipole antenna works as a EMI sensors.

1.4.2. Antenna Factor of a Dipole Antenna

The FDTD model uses a uniform space lattice cubic Yee cells having $\Delta x = \Delta y = \Delta z = 0.8$ cm and $\Delta t = 0.013$ ns. This fine spatial resolution permits direct modeling of the 0.4 cm radius wire, assumed to be PECs. A dipole of length 50 cm and radius 0.4 cm is illuminated by a plane wave of Gaussian impulse of maximum amplitude $A = 1.0$ V/m given by the Eqn. (9) with $t_0 = 0.26666$ nsec and $t_\omega = 0.08$ nsec. Time domain incident linearly polarized electric field $E_z(t)$ is shown in the Fig. 5 and the time domain current $I(t)$ flowing through the center of the dipole is shown in Fig. 3.

Antenna factor of the dipole antenna is evaluated using Eqn. (17). The amplitude part of the complex antenna factor is compared with the published result using MoM [2] shown in Fig. 4. The agreement is quite good considering the different approximations and assumptions made in the FDTD approach related to the MoM, especially in modeling the feed region. Fig. 5 shows the phase part of the complex antenna factor of the dipole antenna.

1.4.3. Antenna Factor of Anritsu MP651A Dipole Antenna

Schematic diagram of a Anritsu MP 651A dipole antenna is shown in the Fig. 6. The length of the antenna is adjustable according to the frequency of operations. The diameter of the arms of the antenna is different for different length. So for a particular frequency mean diameter is taken. The length and mean diameter of the arms of the

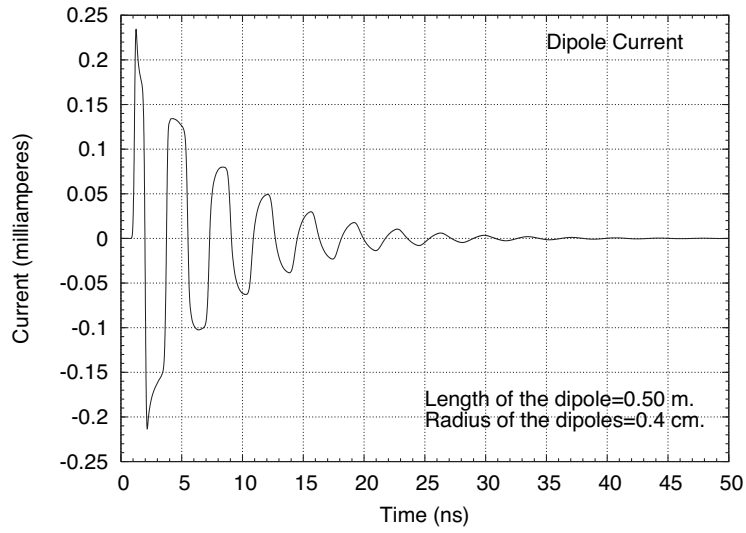


Figure 3. Time domain current flowing through the center of the dipole due to unit amplitude Gaussian plane wave pulse incident on it.

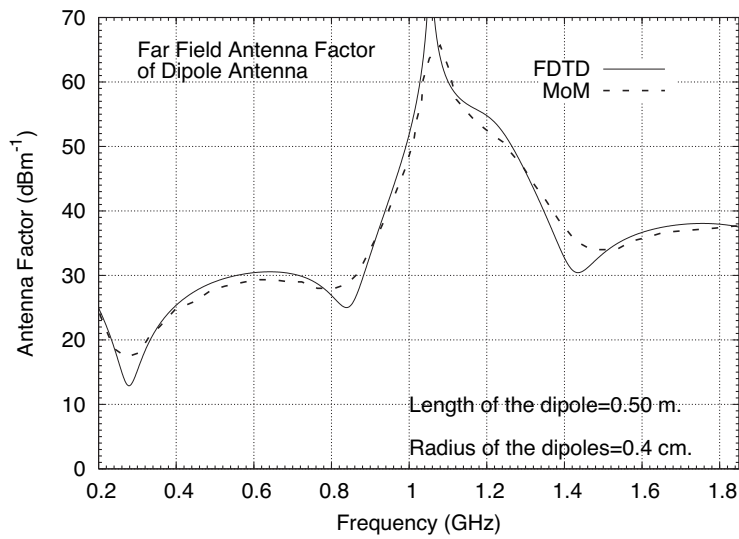


Figure 4. Comparison of the amplitude of the far field complex antenna factor of a dipole antenna using FDTD and MoM results [2].

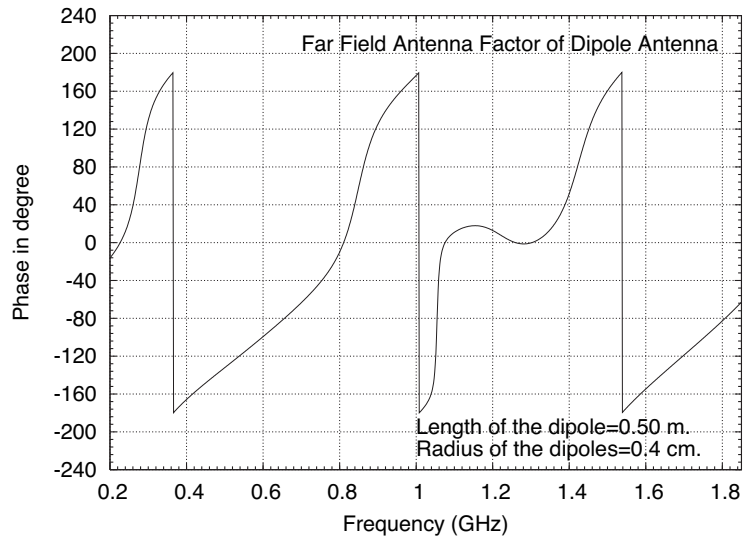


Figure 5. Phase of the far field complex antenna factor of a dipole antenna.

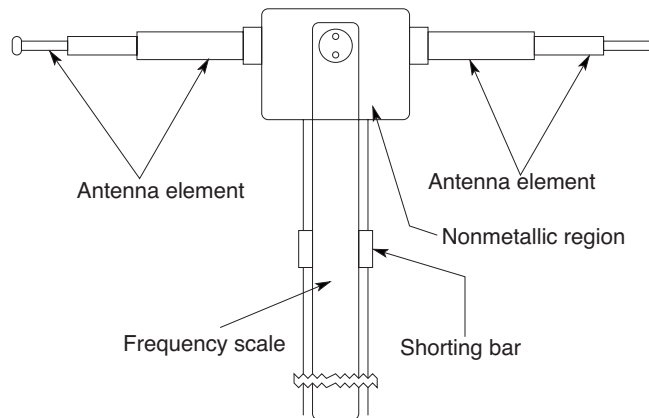


Figure 6. An Anritsu MP651A dipole antenna.

Anritsu dipole were measured for different frequencies and those values were incorporated for numerical evaluation of Antenna Factor, is in Table 1. There are two sets of dipole arms for two different ranges of frequency. One frequency from 470.0 MHz to 1.0 GHz and the other one is from 10 GHz to 1.7 GHz. As length and mean diameter of the dipole are changed with frequency, so frequency separate FDTD simulation is

done for each frequency. For different value of frequency, we perform separate FDTD simulations.

Table 1. Length and mean diameter of the Anritsu MP651A dipole antenna at various frequencies, used for evaluating antenna factor.

Frequency (MHz)	Length (mm.)	Mean diameter (mm.)
470.0	311.12	2.860024
500.0	286.58	3.038269
550.0	257.74	3.266414
600.0	233.02	3.420996
700.0	201.38	3.682818
800.0	157.50	3.795473
900.0	157.50	3.918740
1000.0	140.30	4.062659
1100.0	126.78	3.422933
1200.0	116.54	3.592283
1300.0	106.78	3.796015
1400.0	100.82	3.895904
1500.0	94.42	3.985607
1600.0	88.14	4.092991
1700.0	83.82	4.181545

The FDTD model uses a uniform space lattice cubic Yee cells having $\Delta x = \Delta y = \Delta z =$ diameter of the dipole corresponding frequency. Δt is calculated from Eqn. (8). The free space antenna factor of an Anritsu dipole MP 651A has been evaluated using FDTD and compared with the data available from the chart supplied by the manufacturer [16], is shown in Fig. 7. The agreement is quite good considering the different approximations and assumptions made in the FDTD approach relative to the manual data, especially in modeling the feed region and nonmetallic region shown in the Fig. 6. Phase part of far-field complex antenna factor of an Anritsu MP651A Dipole Antenna is shown in Fig. 8.

1.4.4. Antenna Factor of a Broadband Dipole Antenna

A broadband dipole i.e., dipole loaded with circular disc is shown in Fig. 9. The dimensions of different parts of the antenna are given below:

- Length of the central part of broadband dipole antenna = 0.54 m;

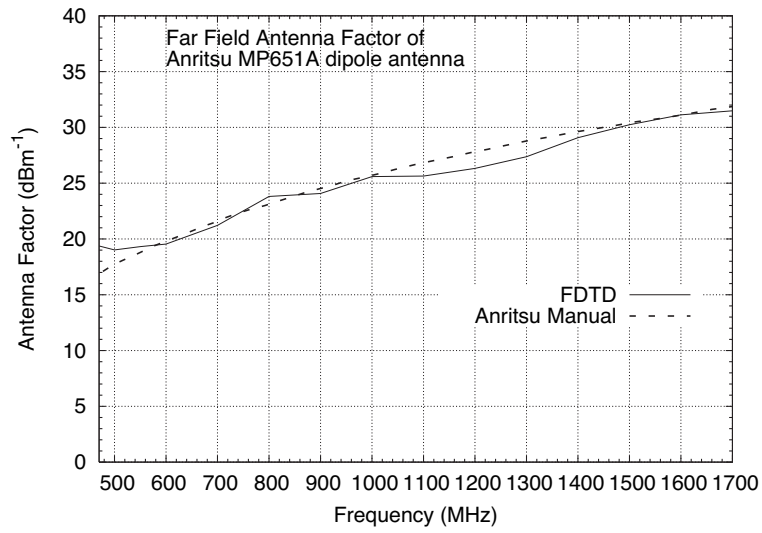


Figure 7. Comparison of antenna factor of an Anritsu MP651A dipole antenna using FDTD and data from Anritsu Manual [16].

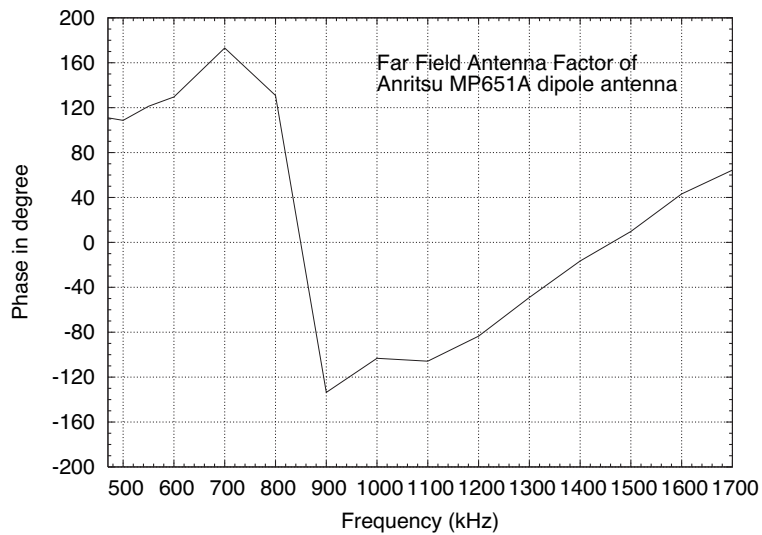


Figure 8. Phase of the far field complex antenna factor of a Anritsu MP651A dipole antenna.

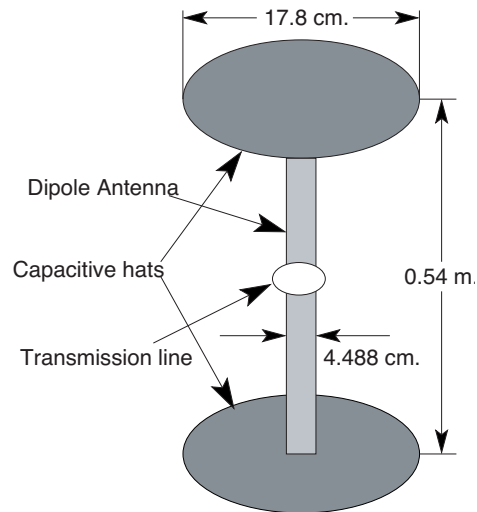


Figure 9. Broadband dipole antenna.

- Radius of the central part of the dipole = 2.244 cm;
- Radius of the capacitive hats = 8.9 cm;

The FDTD model uses a uniform space lattice cubic Yee cells having $\Delta x = \Delta y = \Delta z = 4.488$ cm and $\Delta t = 0.0748$ ns. This fine spatial resolution permits direct modeling of the 2.244 cm radius wire, assumed to be PECs. The dipole is illuminated by a plane wave of Gaussian impulse of maximum amplitude $A = 1.0$ V/m given by the Eqn. (9) with $t_0 = 1.496$ nsec and $t_w = 0.44880$ nsec. Time varying current flowing through the center of the broadband dipole is shown in the Fig. 10. Amplitude of the complex antenna factor of broadband dipole obtained using FDTD has been compared with experimental, MININEC (MoM based commercial software) simulation [3] and MoM based numerical [4, 2] results in Fig. 11. Phase of the complex antenna factor of broadband dipole antenna is shown in the Fig. 12. Considering the differences in how the feed region is modeled the agreement is quite good. FDTD predicted antenna factor is much closer to the experiment result, than the other available in the literature [2–4]. Again within the region, near the frequency 0.1 GHz, FDTD predicted result shows much better agreement with the measurement than the result from MININEC [3] also.

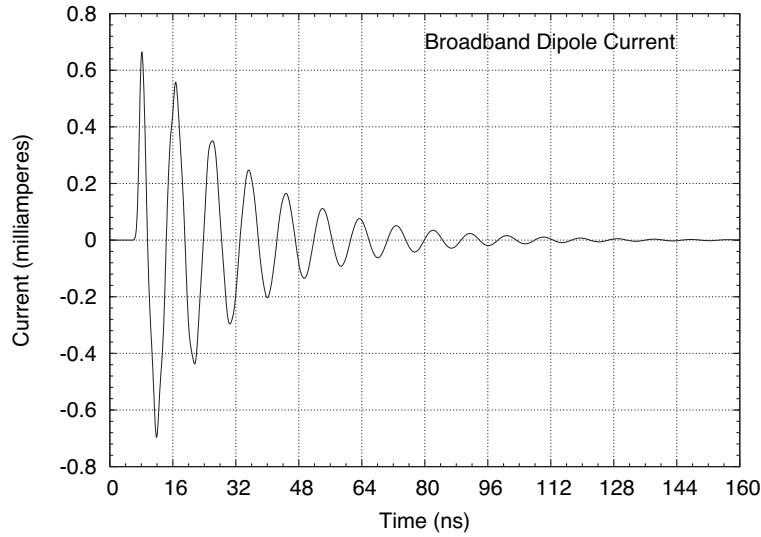


Figure 10. Time domain current flowing through the center of the broadband dipole due to unit amplitude Gaussian plane wave pulse incident on it.

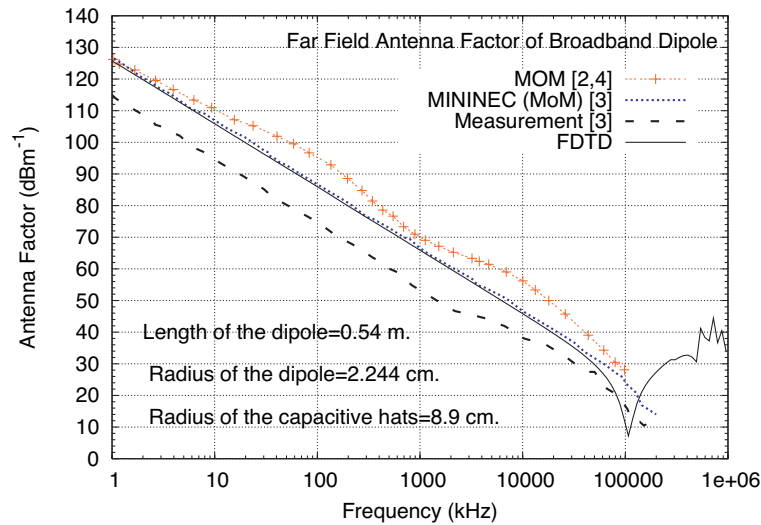


Figure 11. Comparison of the amplitude of the far field complex antenna factor of a broadband dipole using FDTD with published Measurement, MININEC (MoM based commercial software) simulation [3] and MOM based numerical [2, 4] results.

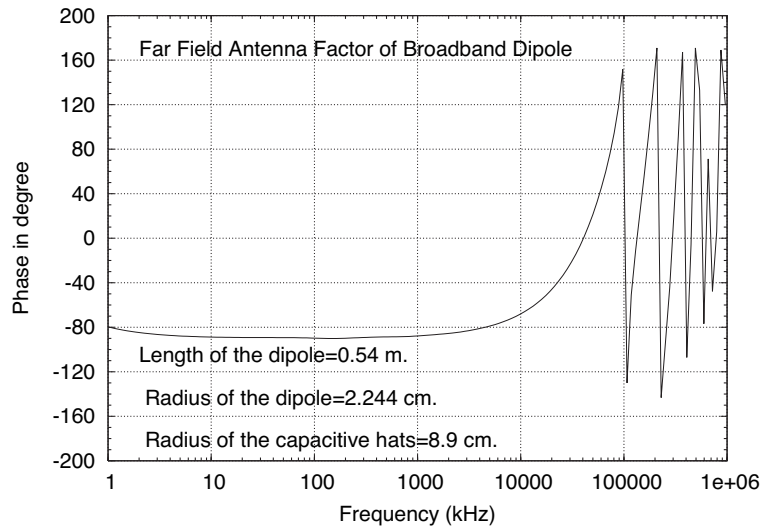


Figure 12. Phase of the far field complex antenna factor of a broadband dipole.

2. DISCUSSION

The FDTD based simulation approach has several advantages over conventional measurement based methods for determining antenna factor.

- Antennas can be illuminated with a plane-electromagnetic wave.
- Time domain current and hence voltage across $50\ \Omega$ load can be calculated.
- Single simulation gives all the frequency components of the results.
- Illumination by a single electromagnetic wave in the direction of bore sight is possible.
- Interactions between antennas and ground planes may be eliminated.

In order to have confidence in any computer model, it must be validated against measurement, but measurements have errors associated with them. It is very difficult to measure plane-wave antenna factor accurately. In the conclusion, it does appear that the manufacturer provided data of antenna factor of the Anritsu MP651A dipole antenna has a significant difference with FDTD simulated results. This is because in the provided data they are not able to eliminate the ground plane effect and also the proper plane wave is not possible to produce in

the measurement. Moreover in the FDTD simulation approach can get both the amplitude and phase from a single simulations where as the manufacturer can provide only the amplitude of the complex Antenna Factor.

FDTD prediction of the antenna factor of EMI sensors is a very attractive alternative if one takes into consideration the enormous expenditure and time required for calibrating a sensor experimentally. Also, for experimental calibration, each and every sensor is to be calibrated individually, whereas for theoretical calibration all the sensors constituting a particular type can be calibrated at one go using the same approach; it is possible to predict the susceptibility of such antennas to electromagnetic radiation incident from any direction. Being time-domain technique, FDTD directly calculates the impulse response of an electromagnetic system. Therefore, a single FDTD simulation can provide either ultra wideband temporal waveforms or the sinusoidal steady state response at any frequency within the excitation spectrum. With FDTD, specifying a new structure to be modeled is reduced to a problem of mesh generation rather than the potentially complex reformulation of an integral equation. For example, FDTD requires no calculation of structure-dependent Green functions. The sources of error in FDTD calculations are well understood, and can be bounded to permit accurate models for very large variety of electromagnetic wave interaction problems. We can easily calculate the near field corrections on far field antenna factor using FDTD method.

3. CONCLUSION

According to the author's knowledge this is the first work where the FDTD technique is used to predict the performance of dipole antenna when it works in receiving mode. For that, firstly, a perfectly plane wave is generated within the FDTD problem space. Then the voltage developed across $50\ \Omega$ load end of the antenna is calculated due to plane wave incident on the antenna. Finally amplitude and phase parts of the complex antenna factor is calculated. Three cases of antenna are considered for the validations of the theory.

Firstly, the antenna factor of a simple dipole is computed. The result is compared with the MoM based numerical [2] results. The agreement is quite good considering the different approximations and assumptions made in the FDTD approach related to the MoM. The FDTD computed phase information of the antenna factor is shown in Fig. 5.

Secondly, the antenna factor of a Anritsu MP651A dipole antenna

is computed. The result is compared with the data available from the chart supplied by the manufacturer [16]. Again the agreement is quite good considering the different approximations and assumptions made in the FDTD approach relative to the manual data, especially in modeling the feed region and nonmetallic region of the Anritsu MP651A dipole antenna system. No phase informations of the complex antenna factor of the Anritsu MP651A dipole antenna is available in the chart supplied by the manufacturer [16]. The FDTD computed phase information of the complex antenna factor of the Anritsu MP651A dipole antenna is shown in the Fig. 8.

Thirdly, the antenna factor of a broadband dipole i.e., dipole loaded with circular disc is computed. Amplitude of the complex antenna factor of broadband dipole obtained using FDTD has been compared with experimental, MININEC (MoM based commercial software) simulation [3] and MoM based numerical [2,4] results. Considering the differences in how the feed region is modeled the agreement is quite good. FDTD predicted antenna factor is much closer to the experimental result, than the other available data in the literature. Again within the region, near the frequency 0.1 GHz, FDTD predicted result shows much better agreement with the measurement than the result from MININEC. The FDTD computed phase information of the complex antenna factor of the broadband dipole antenna is shown in the Fig. 12.

To conclude, we can say that FDTD is very efficient, accurate and easy technique to compute the antenna factor of a dipole antenna. FDTD technique can apply to evaluate error correction factor for the near field case very efficiently, accurately and easily. This technique may be extended to determine the antenna factor of other types of antennas or to study the time domain characteristics of any trans-receive Antenna System [17] when it is other than the free space environment such as for Gigahertz Transverse Electromagnetic (GTEM) Cell of characteristic impedance 50 ohms.

ACKNOWLEDGMENT

The authors would like to acknowledge Dr. S. Ghosh and Prof. A. Chakrabarty for the theoretical discussion time to time.

REFERENCES

1. Paul, C. R., *Introduction to Electromagnetic Compatibility, Wiley Series in Microwave and Optical Engineering*, Wiley, New York, 1992.
2. Ghosh, S., "Some studies on loaded and unloaded wire antennas as EMI sensors," Ph.D. dissertation, Indian Institute of Technology, Kharagpur, Aug. 2003. [Online]. Available: <http://www.ecdept.iitkgp.ernet.in/>.
3. Wang, K. and R. Nelson, "Numerical simulation of the antenna factor of a broadband dipole antenna," *Proc. IEEE International Symposium on Electromagnetic Compatibility*, Vol. 1, 616–619, Aug. 13–17, 2001.
4. Ghosh, S., A. Chakrabarty, and S. Sanyal, "Loaded wire antenna as EMI sensor," *Progress In Electromagnetics Research*, PIER 54, 19–36, 2005.
5. Yee, K. S., "Numerical solution of initial boundary value problems involving maxwells equations in isotropic media," *IEEE Trans. Antennas Propagat.*, Vol. 14, No. 3, 302–307, May 1966.
6. Sullivan, D. M., *Electromagnetic Simulation Using The FDTD Method*, IEEE Press, New York, 2000.
7. Taove, A. and M. Brodwin, "Numerical solution of steady-state electromagnetic scattering problems using the time-dependent maxwells equations," *IEEE Trans. Microwave Theory Tech.*, Vol. MTT-23, No. 8, 623630, Aug. 1975.
8. Sadiku, M., V. Bommel, and S. Agbo, "Stability criteria for finite-difference time-domain algorithm," *Proc. IEEE, Southeastcon*, 48–50, April 1990.
9. Taove, A. and S. C. Hagness, *Computational Electromagnetic—The Finite-Difference Time-Domain Method*, Artech House, Boston, London, 2005.
10. Sullivan, D. M., "A simplified PML for use with the FDTD method," *IEEE Microwave Wireless Compon. Lett.*, Vol. 6, No. 2, 97, Feb. 1996.
11. Sullivan, D. M., "An unsplit step 3-d PML for use with the FDTD method," *IEEE Microwave Wireless Compon. Lett.*, Vol. 7, No. 2, 184–186, July 1997.
12. Yu, W. and R. Mittra, *Conformal Finite-Difference Time-Domain Maxwells Equations Solver: Software and Users Guide*, Artech House, Boston, London, 2004.
13. Das, S. and A. Chakrabarty, "A novel modeling technique to solve

- a class of rectangular waveguide based circuits and radiators,” *Progress In Electromagnetics Research*, PIER 61, 231–252, 2006.
14. Bhattacharya, A., S. Gupta, and A. Chakraborty, “Analysis of rectangular waveguide and thick windows as EMI sensors,” *Progress In Electromagnetics Research*, PIER 22, 231–258, 1999.
 15. Ghosh, S. and A. Chakraborty, “Performance analysis of EMI sensor in different test sites with different wave impedances,” *Progress In Electromagnetics Research*, PIER 62, 127–142, 2006.
 16. *Instruction Manual*, Dipole Antenna MP651A/B, Anritsu Corp, Japan.
 17. Ghosh, S. and A. Chakraborty, “Estimation of equivalent circuit of loaded trans-receive antenna system and its time domain studies,” *Journal of Electromagnetic Waves and Applications*, Vol. 20, 89–103, 2006.